catalysts

MDPI

Article

A Study on the Evaluation Methods of Nitrogen Oxide Removal Performance of Photocatalytic Concrete for Outdoor Applications

Hee-Ju Park [1], Sayed Mukit Hossain [2], Kiin Choi [3], Ho-Kyong Shon [2] and Jong-Ho Kim [1,*]

[1] School of Chemical Engineering, Chonnam National University, Gwangju 61186, Korea; point1014@hanmail.net
[2] Faculty of Engineering and IT, University of Technology, Sydney, P.O. Box 123, Broadway, NSW 2007, Australia; sayed.m.hossain@student.uts.edu.au (S.M.H.); hokyong.shon-1@uts.edu.au (H.-K.S.)
[3] Korea Institute of Ceramic Engineering and Technology, Bucheon 14502, Korea; kichoi@kicet.re.kr
* Correspondence: jonghokim@chonnam.ac.kr

Abstract: In Korea, the issue of particulate matter pollution is growing, and many solutions are being developed to deal with it. Photocatalytic technology has been found to be helpful in removing precursors such as nitrogen oxides that cause particulate matter. In a microcosm setup, ISO 22197-1 has been successfully used to quantify the removal of nitrogen oxides from the specimen to which the photocatalyst is applied. However, owing to a lack of suitable tools, on-site measurement of real-scale efficacy is difficult. Depending on the substrate and surrounding circumstances at the application location, the photocatalyst may function at varying levels. Additionally, the expected photocatalytic effect may differ depending on the ambient air quality and sunlight irradiation intensity. This article describes two approaches for studying outdoor concrete photocatalysis. Standard gas measurement and dual-reactor measurement are the recommended evaluation approaches. The standard gas measurement method was found useful for assessing the applied photocatalyst itself as an outcome of field assessment. The performance of photocatalysts at different sites was found to be mutually exclusive and comparable. Over 180 min, on a building roof deck, the NO removal by the standard gas method was 0.68 ppm, whereas, at two shaded locations, the removal amount was 0.51 ppm (side wall) and 0.24 ppm (underpass) for 300 min. The dual reactor measurement approach, on the other hand, was discovered to be one of the most suitable methods for assessing how much of an improvement there has been in the air quality in areas where photocatalysts have been placed.

Keywords: photocatalyst; nitrogen oxide; ISO 22197-1; NO removal; outdoor test; real-time data

Citation: Park, H.-J.; Hossain, S.M.; Choi, K.; Shon, H.-K.; Kim, J.-H. A Study on the Evaluation Methods of Nitrogen Oxide Removal Performance of Photocatalytic Concrete for Outdoor Applications. *Catalysts* **2022**, *12*, 846. https://doi.org/10.3390/catal12080846

Academic Editors: Hugo de Lasa and Salvador Escobedo

Received: 4 July 2022
Accepted: 28 July 2022
Published: 2 August 2022

1. Introduction

Particulate matter is becoming a critical problem in Korea. According to the 2020 Environmental Performance Index announced by the World Economic Forum in Davos, Switzerland, it ranked 28th out of 180 countries. However, it is ranked 45th in particulate matter exposure in the environmental health sector [1]. Particulate matter is generated from the secondary reaction of gaseous precursors, and these precursors include nitrogen oxides (NO_x), sulfur oxides (SO_x), ammonia (NH_3), and volatile organic compounds (VOCs) [2–8]. Although the harmfulness of particulate matter is high, it is known that the harmfulness of the precursors is also high. In particular, NO_x causes problems such as acid rain, photochemical smog, ozone layer destruction, greenhouse effect, and ecotoxicity [7,9–12]. Of these harmful precursors, NO_x can be removed through photooxidation [5–8,13–16]. Photocatalyst-incorporated concrete products for removing low-concentration NO_x in the atmosphere by utilizing this reaction are being studied comprehensively [10,17–20]. Recent research into the NO_x removal effectiveness and durability of photocatalyst-based building materials has produced ways for evaluating quantitative findings in outdoor settings

for more practical applications [21–25]. Guerrini [26] demonstrated the outcomes of two environmental monitoring programs, including examining NO_x levels recorded before and after the renovation of Rome's "Umberto I" tunnel and analyzing the NO_x removal ability of photocatalytic cement-based paint. Guerrini's studies suggest that photocatalytic treatment of the Umberto I tunnel vault with cementitious paint resulted in significant pollution reduction, as seen by the lower quantities discovered after the restoration. Maggos et al. [27] conducted a field investigation by constructing an artificial roadway canyon with a width-to-height ratio of 0.4 and a high input NO concentration generated by a gas generator. Depending on airflow and road direction, the NO_x removal efficiency ranged from 36.7% to 82.0%. Later, Boonen and Beeldens [22] indicated that translating laboratory findings to the actual site remains challenging due to the vast number of factors. Moreover, large-scale projects to establish the effectiveness of photocatalytic materials are vital.

Yu et al. [28] looked into the performance of a mineral-based translucent air-purifying paint. The ISO 22197-1 procedure was used to test the efficacy of this photocatalytic paint for eliminating air pollutants in a laboratory environment. Following that, outdoor testing was carried out over 20 months to establish the effectiveness of air pollution removal under actual settings. They presented a novel procedure for monitoring air pollutant removal effectiveness based on the observed nitrate (NO_3^-) generated by nitrogen oxide's photocatalytic oxidation. de Melo et al. [29] tested the efficacy of photocatalytic pavement in the field for 1 year in Brazil and reported a significant decline in NO_x degradation efficiency over time. In the Netherlands, Ballari and Brouwers [30] completed a comprehensive demonstration project using the air-purifying pavement. When the photocatalyst is placed as a surface coating on paving stones, they find a rapid drop in NO_x degradation efficiency. Folli et al. [23] conducted a field test of TiO_2-containing air-purifying pavement materials. In contrast to a very high lab NO degradation of over 78%, they found that under optimal weather circumstances (i.e., midsummer), the monthly average NO concentration was approximately 22% lower than in the reference location. Cordero et al. [31] used two pilot-scale demonstration platforms built at two different sites to assess the NO_x removal performance of 10 distinct materials. The materials were left outside for over a year, and the concentrations of NO and NO_2 in the environment were measured. By comparing the pollutant removal effectiveness of the materials to concurrently measured concentrations of reference materials, the pollutant removal rate of the materials was calculated. Gallus et al. [25] conducted a photocatalytic de-pollution field experiment in Brussels' Leopold II tunnel. Between June 2011 and January 2013, three monitoring programs were conducted. The tunnels' sides and ceilings were coated with a photocatalytically activated coating. The field results, in contrast to the laboratory results, indicated no substantial decrease in NO_x in the tunnel test. Furthermore, a significant deactivation of the photocatalytic material was detected beneath the extremely polluted tunnel. The preceding literature reveals the following distinguishing features:

- As seen by the very variable performance of photocatalytic coatings in diverse field investigations, environmental variables critically impact the efficiency with which photocatalytic coatings degrade NO_x. However, in laboratory circumstances, such coatings demonstrate excellent efficiency.
- Designing a viable field monitoring methodology, as well as assessment methodologies, is challenging.

In general, ISO 22197-1 (Fine ceramics (advanced ceramics, advanced technical ceramics)—Test method for air-purification performance of semiconducting photocatalytic materials—Part 1: Removal of nitric oxide) was enacted and is utilized as a method for evaluating the photocatalyst applied specimen [32]. However, it is not possible to confirm the actual effect of photocatalytic concrete installed outdoors in this way. The present work aimed to devise and set up a simple experimental apparatus for evaluating the photocatalytic performance of materials in actual outdoor situations, where NO_x content and solar irritation are the variables.

2. Results and Discussion

2.1. Application of Standard Gas Measurement Method

In this study, the same photocatalytic coating agent (Bentech Frontier product using photocatalyst coating (ZT-01)) was applied to the selected locations (Figure 1) to evaluate the application of the standard gas measurement method. The photocatalyst coating agent was applied by first using a primer and then applying a photocatalyst in the same way that a general paint was applied to the concrete surface. The outdoor standard gas measurement was carried out in three locations, the first being the roof deck (Figure 1a) of the building and the other two being the wall (Figure 1b,c) of the building.

Figure 1. NO_x removal measurement locations in real-time at (**a**) the roof of the building (Gwangju Chonnam University Hall 5), (**b**) wall of the underpass (West Pyeongju Underground Carriageway, Daegu), and (**c**) exterior wall of the building (Gerryeo-dong Apartments, Seoul, South Korea).

For the experiment, the incoming NO_x gas was supplied at a concentration of 3.0 ppm, a flowrate of 3.0 L/min, and a relative humidity of 50% [32]. The NO_x concentration discharged from the reactor was measured along with the amount of UV light irradiated by sunlight at the place where the reactor was installed. Figure 2 shows the performance of the photocatalyst applied to the roof of the building, as measured by the standard gas measurement method.

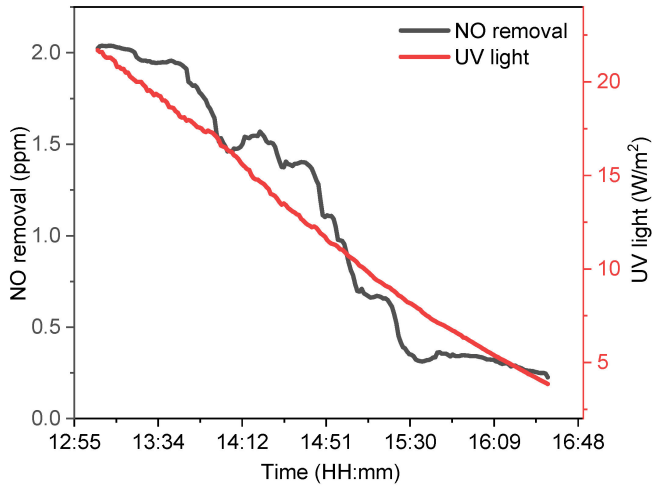

Figure 2. Performance result of photocatalyst applied to the roof of a building.

As shown in Figure 2, the amount of sunlight irradiated decreases as the sun's altitude decreases with time, starting from 1.06 p.m. to 4.06 p.m. As a result of the measurements that were taken on the roof deck of the building, it was determined that the intensity of the sun's irradiation was satisfactory and that during the course of the experiment, the minimum intensity of the UV light was at least 4 W/m^2. The maximum amount of irradiated light was 21.7 W/m^2, and the NO removal amount under the maximum amount of light was 2.02 ppm, the most elevated removal amount. Figure 3 depicts the results of measurements on the photocatalyst applied to the building's sidewall, which illustrates a circumstance in which sunlight is disrupted by the neighboring structures. The duration of the photoactivity assessment on the side wall was well distributed within 9.00 a.m. to 3.00 p.m.

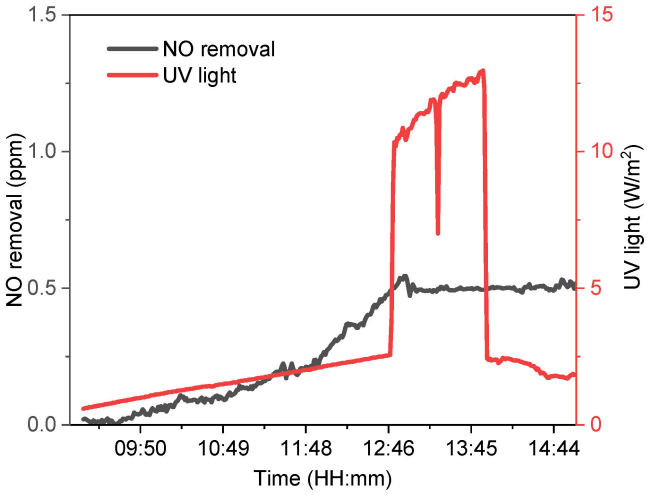

Figure 3. Measurement result of photocatalyst applied to the side of the building.

From Figure 3, it can be seen that the UV light irradiation intensity of sunlight was low at the beginning of the day, but the irradiation intensity increased for a certain period, and the irradiation amount of the sun rapidly decreased after a specific time. When the above change in light intensity is reflected in the field conditions, the photocatalyst coating surface is shaded by other nearby buildings, and the amount of light intensity is less than 3 W/m^2. After a specific time, sunlight was not directly introduced but in the form of reflected light, and the amount of light intensity was continued at 3 W/m^2 or less again. It can be confirmed that when the amount of sunlight increases, the activity of the photocatalyst increases, and after the maximum photocatalytic activity is reached, it can be demonstrated that the photocatalytic activity does not show a significant change even when the amount of sunlight increases around midday (12.40 p.m. to 2.00 p.m.). In addition, it appears that the photocatalytic activity is maintained even under the condition where no direct light is irradiated (after 2.00 p.m.), which is believed to be affected by the photocatalyst activity by indirect light, which is not measured at an angle on the installed UV photometer. Figure 4 shows the photocatalyst's performance results applied to the underpass's entrance wall. As shown in Figure 4, the maximum light intensity was 18.8 W/m^2 (around midday), and it can be confirmed that the overall sunlight irradiation conditions were good. It is considered that only changes in the amount of sunlight irradiated by clouds are reflected. Despite good sunlight irradiation conditions, the maximum removal amount was 0.27 ppm, which was considered to exhibit very low photocatalytic activity. The cumulative removal of NO during the measurement time to compare photocatalyst activity of the same photocatalyst coating was applied to different spaces. The removal of NO under the UV light condition of ISO 22197-1, and the average irradiation light level of sunlight irradiated on the coating surface, was summarized in Table 1.

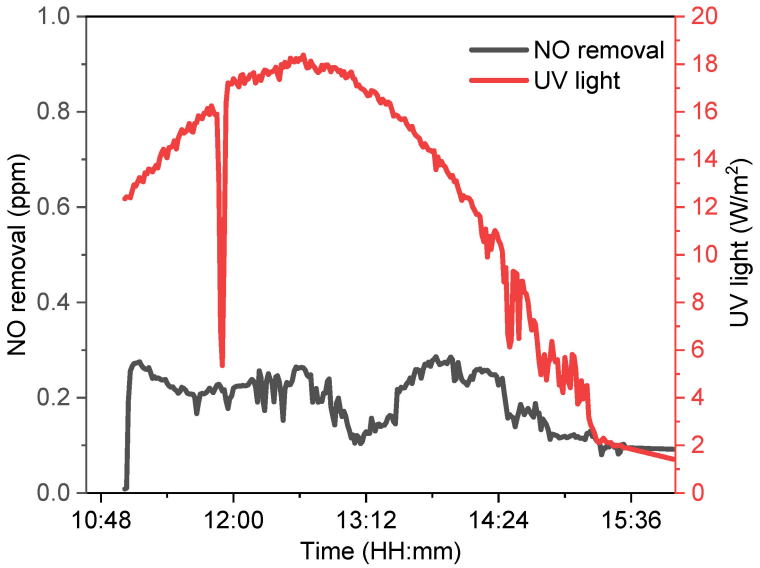

Figure 4. Performance result of photocatalyst applied to the wall of the underpass entrance.

Table 1. Photocatalyst activity at evaluated locations, measured by the standard gas measurement method.

Location	Total Time (min)	Cumulative NO Removal (μmol)	Average Sun Light Intensity (W/m^2)	Removal Amount (10 W/m^2 Condition)
Building roof deck surface	180	24.48	12.2	0.68 ppm
Building side wall	300	11.06	3.5	0.51 ppm
Underpass entrance wall	300	6.99	12.8	0.24 ppm

From the assessment results at a specific place to which the photocatalyst is applied, it can be seen that the photocatalytic activity tends to increase when the amount of sunlight is increased. However, as shown in Table 1 above, it can be seen that there is a significant difference in activity between the floor surface of the building's roof and the wall of the underground passageway when there are similar light conditions. This shows that even if the same photocatalyst coating agent is applied, the activity of the photocatalyst may vary depending on the location and type of the substrate. In addition, even in the case of a substrate coated with a photocatalyst exhibiting low activity, it was confirmed that the NO removal amount was low still when the amount of sunlight irradiation was high. With this standard gas measurement method, it can be confirmed that the photocatalyst applied to different spaces differs in the amount of NO removed, depending on the site conditions and the maximum photocatalytic activity of the exterior building surface to which the photocatalyst is applied. In addition, it is considered that the weather resistance of the applied photocatalyst can be evaluated by following the same coating surface. However, since the experiment is conducted with standard gas, only the activity of the photocatalyst in relation to the quantity of light can be determined; therefore, the real NO oxidation rate in the field cannot be calculated.

2.2. Result of Application of Dual Reactor Measurement Method

In the second study, to test the application of the dual reactor measurement method, the experiment was conducted on the wall of the underground passageway (West Pyeongju Underground Carriageway, Daegu) where the photocatalytic coating was applied. Figure 5 shows the NO concentration measurement results under light conditions and the NO

concentration measurement results under dark conditions, measured from the wall of the underpass entrance. In addition, the amount of sunlight irradiated at the measurement time was also assessed.

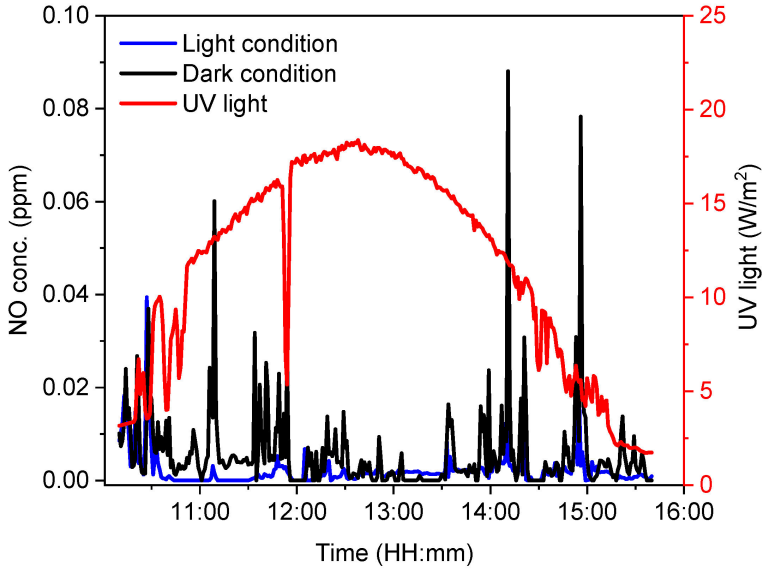

Figure 5. Dual reactor measurement result (Location: West Pyeongju Underground Carriageway, Daegu; Date: 19 December 2019).

Two measuring instruments were calibrated using standard gas before the investigation in the dual reactor measurement method. A preliminary measurement was performed for 15 min with the light and dark reactors set to the same dark conditions in the calibrated state. Under the dark conditions, the values of the two measuring instruments showed a difference of 0.001 ppm on average and 0.0005 in the cumulative amount of NO, confirming that the error of the measuring instruments was not substantial. After 15 min, the light condition reactor was set up so that sunlight could be irradiated, and the experiment was carried out. In the dark conditions, it was confirmed that the in situ atmospheric concentration was measured in the reactor, and the NO concentration changed according to the type and number of vehicles entering the underpass. In addition, the intake concentration appeared to be at a level where the concentration of NO was hardly measured in the state of no vehicle operation, and the maximum concentration of NO was recorded at 0.088 ppm. In the aforementioned experiment, when measuring the light conditions, the maximum amount of UV light from sunlight was 18.18 W/m^2, the average light intensity was 11.66 W/m^2, and the irradiation conditions were deemed very promising. Under the same dark conditions, the NO emission concentration of the reactor did not show a significant difference. Still, when sunlight was irradiated into the light-conditioned reactor, the NO concentration of the dark-conditioned reactor and the light-conditioned reactor started to differ by 0.0341 (see Table 2) and was shown on the photocatalyst application surface with an area of 150 cm^2 during the measurement time. This removal amount was calculated to show a removal rate of 70.7% compared to the NO concentration in the surrounding air when it was converted into a removal rate. Additionally, Figure 6 and Table 3 show the measurement results using the dual reactor measurement method at the exact location but on a different date as the measurement location in Figure 5.

Table 2. Preliminary data comparison of the dual reactor measurement method for a 15 min time step (Location: West Pyeongju Underground Carriageway, Daegu; Date: 19 December 2019).

Irradiation State	15 min (Before)		15 min (After)		η_{NO} (μmol)	NO Removal Rates (%)
	Average Concentration (ppm)	NO Total Amount (μmol)	Average Concentration (ppm)	NO Total Amount (μmol)		
Dark	0.0118	0.0068	0.0055	0.0482	0.0341	70.7
Sun light	0.0108	0.0063	0.0016	0.0141		

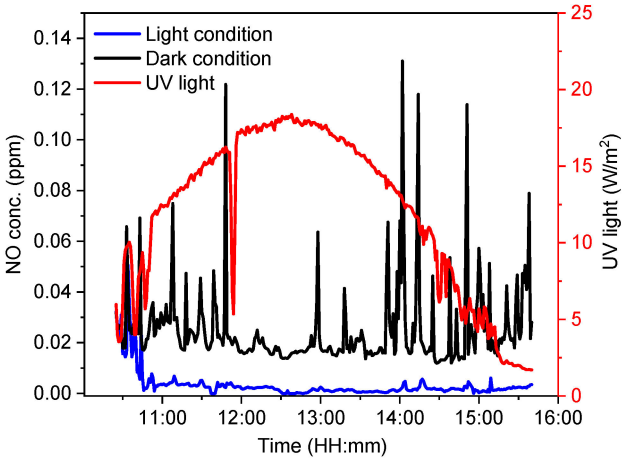

Figure 6. Dual Reactor Measurement Result (Location: West Pyeongju Underground Carriageway, Daegu; Date: 4 February 2020).

Table 3. Data comparison of the dual reactor measurement method for a 15 min time step (Location: West Pyeongju Underground Carriageway, Daegu; Date: 4 February 2020).

Irradiation State	15 min (Before)		15 min (After)		η_{NO} (μmol)	NO Removal Rates (%)
	Average Concentration (ppm)	NO Total Amount (μmol)	Average Concentration (ppm)	NO Total Amount (μmol)		
Dark	0.0284	0.0124	0.0249	0.2171	0.198	91.2
Sun light	0.0246	0.0108	0.0022	0.0191		

During the measurement time, the NO removal amount from the 150 cm^2 area of the photocatalyst application surface was 0.198 μmol. When converted into a removal rate, it shows a high value of 91.2%. Compared to the primary measurement result, the concentration of incoming NO was high, but the removal rate was higher. During the measurement depicted in Figure 6, the sunlight irradiation conditions showed that the maximum amount of UV light was 18.38 W/m^2. The average light amount was 12.03 W/m^2, which is higher than the first experiment's sunlight irradiation conditions. Therefore, it can be considered that the increase in the NO removal rate is due to the rise in the amount of UV light along with the increase in NO concentration. In this measurement period, it can be seen that even under the condition of low vehicle traffic, the NO measured value in the dark state does not show at least 0.17 ppm or less, unlike the measurement performed on 19 December 2019. Hence, it can be evaluated that the NO concentration within the reactor was high.

Figure 7 depicts the photocatalytic activity of the exact location as Figure 6, determined using the dual reactor measurement technique, but on the subsequent 5 February 2020 (see Table 4). After the following measurement period had passed, the quantity of NO that had been removed from the 150 cm^2 area of the photocatalyst application surface was found to be 0.107 μmol. When turned into a removal rate, the high value of 83.2%

was confirmed. When the circumstances of sunlight irradiation were analyzed, it was determined that the most significant amount of ultraviolet light was 13.12 W/m^2, and the average light amount was 6.3 W/m^2, which was practically half the level of the sun intensity that was recorded on 4 February 2020. In light of the cloudy weather, it has been established beyond a reasonable doubt that the NO removal rate is greater than the result of the primary measurement (which was carried out on the 19th of December 2019). This disparity in removal rates is believed to be the result of a distinction in the pattern of change in the NO concentration that was fetched in from the outside. Regarding the preliminary measurement, the variation in the abrupt inlet concentration that occurs based on the driving circumstances of the vehicle is substantial.

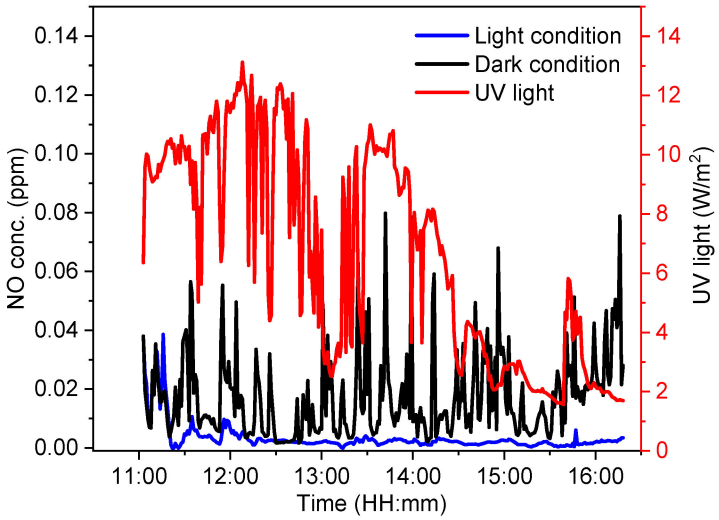

Figure 7. Dual reactor measurement result (Location: West Pyeongju Underground Carriageway, Daegu; Date: 5 February 2020).

Table 4. Data comparison of the dual reactor measurement method for a 15 min time step (Location: West Pyeongju Underground Carriageway, Daegu; Date: 5 February 2020).

Irradiation State	15 min (Before)		15 min (After)		η_{NO} (μmol)	NO Removal Rate (%)
	Average Concentration (ppm)	NO Total Amount (μmol)	Average Concentration (ppm)	NO Total Amount (μmol)		
Dark	0.0195	0.0085	0.0147	0.1283	0.1067	83.2
Sun light	0.0228	0.0100	0.0025	0.0216		

In contrast, in the case of the measurement illustrated in Figure 7, a specific concentration or more is maintained. In addition, it is evaluated that the photocatalytic activity is maintained even at 1–2 W/m^2 of light by looking at the solar irradiation conditions and the removal tendency at the end of the measurement performed on 5 February 2020. In general, it is considered that the difference in photoactivity does not occur significantly when a certain amount of light is irradiated. As a result of operating the dual reactor measurement method for outdoor sites where photocatalyst coatings were applied, it was confirmed that the evaluation reflects the ambient condition and solar irradiation conditions of the site where the photocatalyst was used. In addition, it is reckoned that the effect of photocatalyst application can be evaluated as the actual NO removal amount and removal rate are derived for improving air quality. It cannot be assessed by cross measurements other than at the same location because it is a method of measuring using the atmospheric environment and sunlight of the site. In the case of securing primary data by selecting representative sampling locations, it is thought that this data can be used to determine the overall air quality improvement effect of the site where the photocatalyst is applied.

3. Materials and Method

3.1. Derivation of Outdoor Photocatalyst Evaluation Method

Currently, the most commonly used method to evaluate the NO_x removal activity of a product to which a photocatalyst is applied is the ISO 22197-1 [32] method. This evaluation method is commonly used to confirm the NO_x removal properties of ceramic materials to which a photocatalyst is applied. Figure 8 shows the experimental schematic of ISO 22197-1.

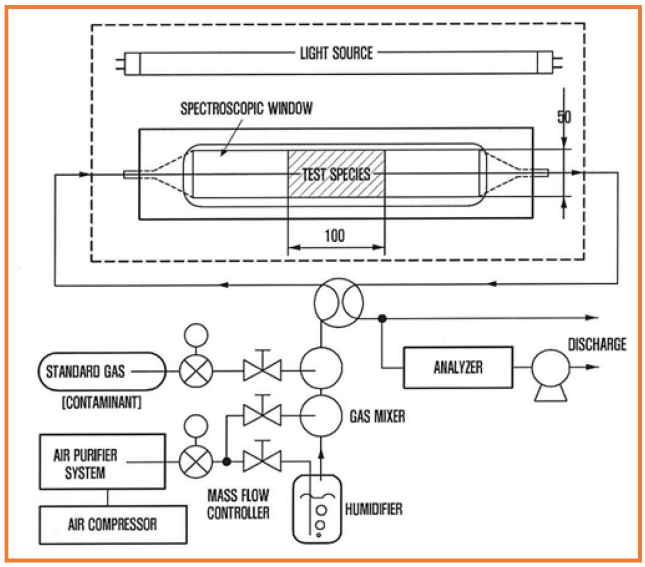

Figure 8. ISO 22197-1 Experimental Equipment Schematic.

The ISO 22197-1 method stipulates that the range of test specimens that can be tested is the flat plate, board, and honeycomb types specified in this standard, and powder or granules are not applied [32]. Therefore, the method of ISO 22197-1 cannot evaluate the photocatalytic activity of the photocatalyst product installed in the field. This study devised two methods to evaluate photocatalytic concrete products applied outdoors by applying ISO 22197-1. The first method is to perform the same test as ISO 22197-1 but change the process of attaching the reactor and the light source. To measure the sample applied outdoors, where it is impossible to cut the sample, we devised a method to attach only the upper surface of the reactor to the surface to which the photocatalyst is applied. Other conditions are the same as in ISO 22197-1, and the method was named the "standard gas measurement method" in this experiment. The second method is to configure the reactor and light source conditions the same way as the first method. Instead of injecting NO_x standard gas at a specific concentration, as in ISO 22197-1, it is a method of injecting the actual atmospheric NO_x and allowing it to pass through the reactor. To confirm the photocatalytic reaction, the photocatalytic activity is evaluated by attaching and measuring a dark-condition reactor of the same size and checking the concentration difference between the two reactors. The second devised method was named the "dual reactor measurement method" in this experiment.

3.2. Outdoor Measuring Device Arrangements

The standard gas measurement method consists of a reactor attached to the photocatalyst applied surface, a gas supply device that can supply standard gas with constant humidity and concentration, and an analyzer analyzing NO_x. The reactor used in this study is measured by attaching it differently to the sample than the existing ISO reactor. Hence, it was configured differently than the existing reactor. In the case of the current ISO 22197-1 reactor, a flow path with a width of 50 mm is secured, and a space for placing a sample is confirmed at 100 mm. As shown in Figure 8, 100 mm is ensured at the front end

of the sample and 100 mm is secured at the rear end of the sample so that the total size of the reactor is 300 mm. Therefore, the size of the entire visible window should be at least 300 mm × 50 mm. The size of the applied sample is 100 mm × 50 mm and the thickness is 10 mm. The distance between the specimen and the visible window is maintained at 5 mm so that the test gas can flow, and a quartz window with a low UV blocking rate is used for the visible window. Figure 9 shows the attached reactor designed in this study. The distance between the attachment surface and the visible window was maintained at 5 mm, and the material of the visible window was composed of quartz window in the same way as ISO 22197-1. The size of the visible window was 300 mm × 50 mm. However, all areas irradiated under the visible window become the sample area. Therefore, the cross-sectional area of the sample was estimated as 300 mm × 50 mm.

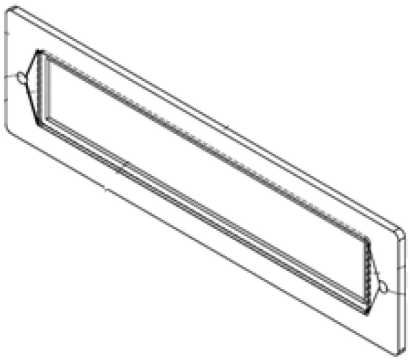

Figure 9. Experimental Reactor Schematic.

The gas supply device for supplying standard gas with constant humidity and concentration is based on the gas supply device in the schematic diagram of Figure 10, which shows the conceptual diagram of the manufactured external standard gas supply device.

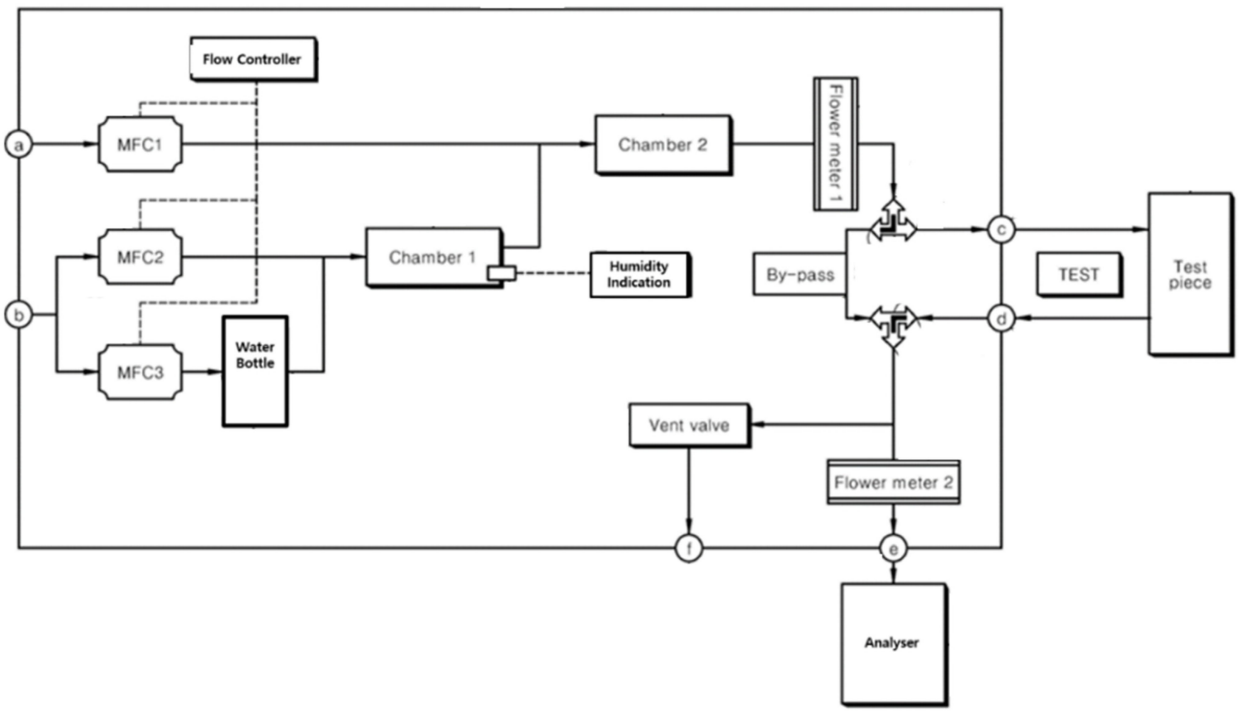

Figure 10. Conceptual drawing of outdoor standard gas supply system.

As shown in Figure 10, the outdoor standard gas supply device consists of a standard gas inlet and a general air inlet, and the humidity is controlled by controlling the amount

of wet and dry air in the air inlet. The mixed gas is mixed with this air and controls the supplied standard gas concentration. A mass flow controller regulates the amount of standard gas and air introduced, and a separate flow meter is installed to check the flow rate before entering the reactor. The gas that has passed through the reactor is sampled in an amount required for the analyzer, and the remaining gas is discharged. The NO_x analyzer used in this study is Ecotech's Serinus 40 model, and this model can measure NO, NO_2, and NO_x continuously. The concentration measurement range is 0–20 ppm, the measurement limit is 0.4 ppb, and the ambient temperature range is 0 °C to 40 °C. For the measurement of light irradiation, a UV photometer (YK-37UVSD) (Delta Ohm, Padua, Italy) was utilized with wavelength measuring limits of 280 to 390 nm.

3.3. Outdoor Measurement Methods

As mentioned above, two outdoor photocatalyst measurement methods were devised, and they were named the standard gas measurement method and the dual reactor measurement method. Figure 11 shows a schematic diagram of the standard gas measurement method. The standard gas measurement method measures the amount of NO removed by the photocatalyst after injecting a specific concentration of NO gas into the reactor in the same way as ISO 22197-1. Figure 11 shows how the reactor is attached to the photocatalyst applied surface where measurement is needed. Under the condition that standard gas is supplied, the experiment is conducted using outdoor sunlight without a separate light source. The amount of NO gas removed is calculated by calculating the difference between dark and light conditions in the same way as in ISO 22197-1. The experiment is conducted based on the initial concentration value for the concentration measurement under dark conditions. The installed reactor was operated under dark conditions without installing a separate dark-condition reactor. The amount of NO removed by the photocatalyst in the standard gas measurement method is calculated by Equation (1).

$$n_{NO} = \left(\frac{f}{22.4}\right) \int_0^t (\phi_{NO_i} - \phi_{NO})\, dt \quad (1)$$

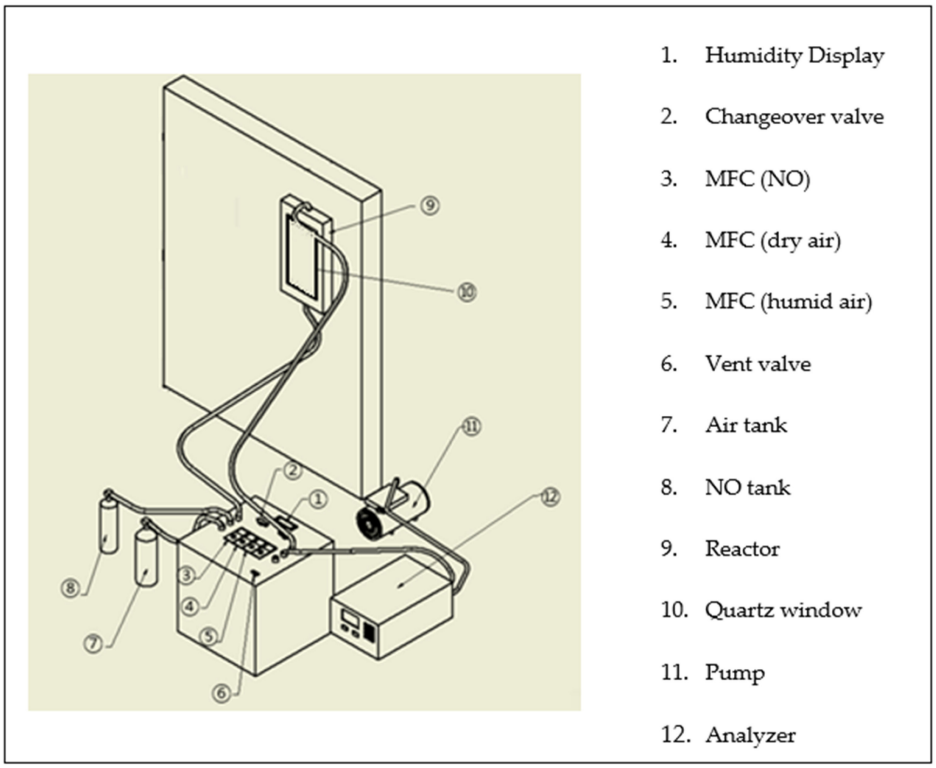

Figure 11. Standard gas measurement method.

Here,

n_{NO}	Amount of Nitric Oxide Removed (μmol)
f	Air flow rate converted to standard condition (0 °C, 101.3 kPa, based on dry gas) (L/min)
ϕ_{NO_i}	Initial supply rate of nitrogen oxide (μL/L)
ϕ_{NO}	Rate of volume of nitrogen oxide at outlet (μL/L)

Figure 12 shows a schematic diagram of the dual reactor measurement method. In the dual reactor measurement method, two reactors are installed on the application side to which the photocatalyst is applied, as shown in Figure 12, and one installed reactor is measured under light conditions and the other under dark conditions. A black plastic cover was utilized to cover the quartz window of the reactor to prevent the sunlight from entering. The incoming gas uses atmospheric air and the light source utilizes sunlight. The amount of NO removed by the photocatalyst in the dual reactor measurement method is measured using Equation (1). However, since the NO concentration in the incoming atmosphere changes differently from the standard gas, the nitrogen oxide inflow volume is calculated based on the measured value under dark conditions.

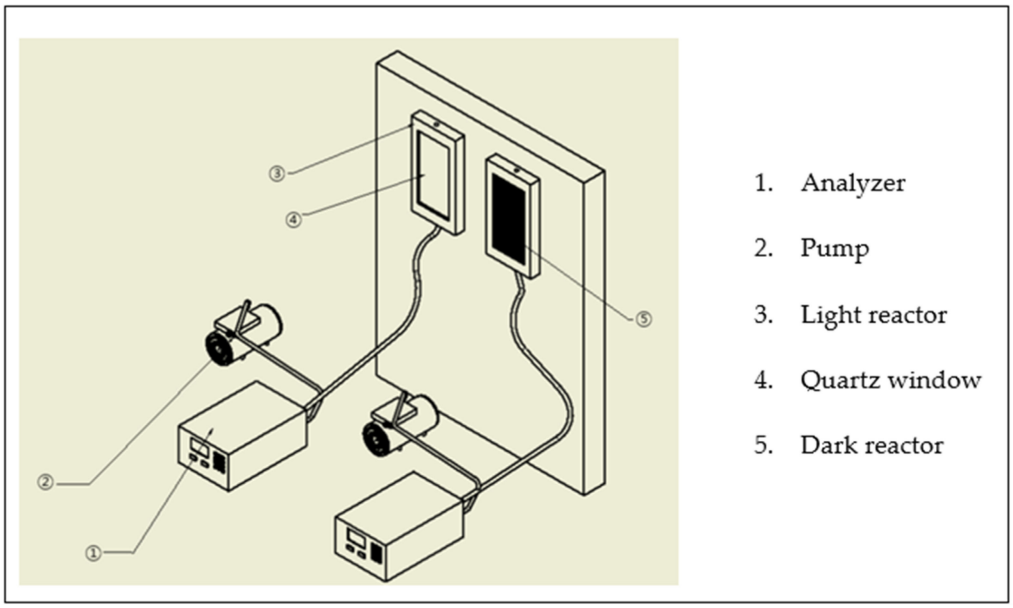

Figure 12. Dual reactor measurement method.

3.4. Photocatalyst Application and Characterization

This study utilized the commercially available photocatalytic coating ZT-01 from Bentech Frontier (Jangseong-gun, South Korea). Using the spray coating method, the studied sites shown in Figure 1 were coated with three coating layers. The chemical composition of the commercial ZT-01 is illustrated in Table 5. As shown in Table 5, the primary component contributing to the photocatalytic activity is the anatase TiO_2 incorporated into the coating solution. A field emission scanning electronic microscope (FESEM; S44700, Hitachi, Tokyo, Japan) at a working distance of 7 mm and 10 kV in a vacuum was employed to study the morphology of the photocatalyst incorporated into ZT-01. The fundamental constituents of the photocatalyst were evaluated using the EDS detector (55VP SEM) running at 10 kV. The FESEM image and the EDS representations are depicted in Figure 13. Moreover, the elemental composition from the EDS mapping is tabulated in Table 5. The composition of the photocatalytic material in wt.(%) was found as C (1.97%), O (44.11%), Ti (52.91%), and Zr (1.01%).

Table 5. Elemental composition of ZT-01 and the incorporated photocatalyst based on the EDS mapping.

ZT-01		Photocatalyst		
Elements	**Proportion (wt.%)**	**Elements**	**Proportion (wt.%)**	**Proportion (Atomic%)**
Anatase TiO_2	1.75%	C	1.97	4.05
C_2H_5OH	41.6%	O	44.11	68.31
H_2O and others	51.05%	Ti	52.91	27.36
		Zr	1.01	0.27

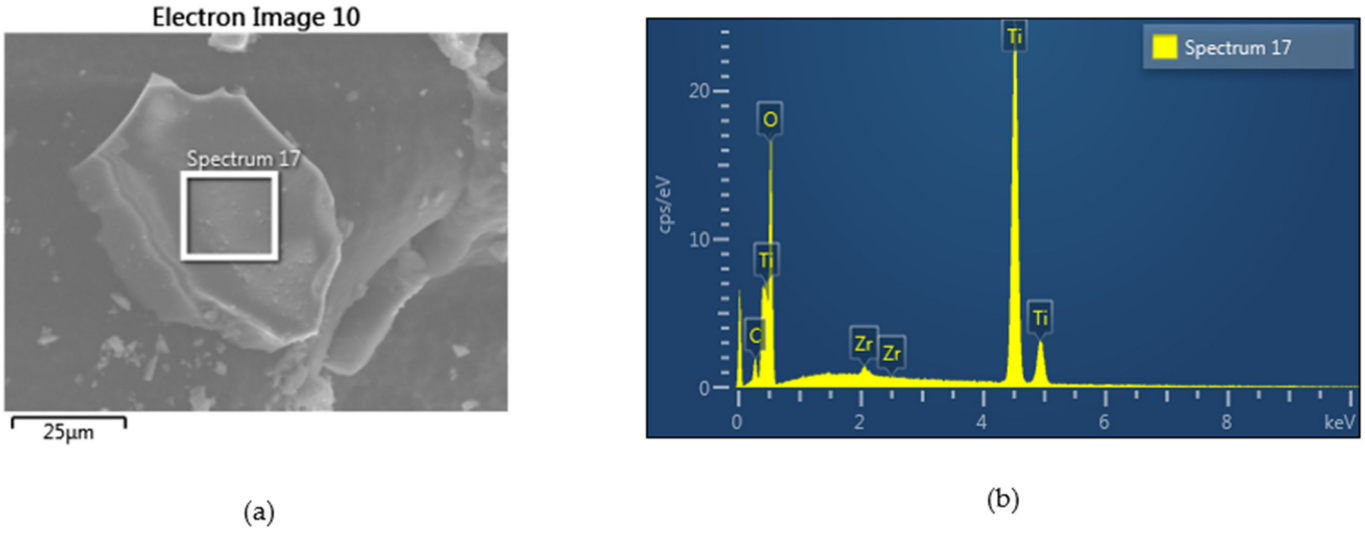

Figure 13. (**a**) Field emission scanning electronic microscope (FESEM) image of ZT-01, (**b**) EDS spectra.

3.5. NO Removal Mechanism

A number of our previous studies have already established the atmospheric NO removal mechanism of UV-induced TiO_2 [5–8,12,33]. Upon UV irradiation, the photocatalysts get excited and generate electron-hole pairs (e^-/h^+). Later, the photogenerated e^- on the conduction band (CB) reduces the surrounding adsorbed oxygen to superoxide ($\cdot O_2{}^-$) and the h^+ on the valence band (VB) oxidizes $H_2O(OH^-)$ into hydroxyl ($\cdot$OH) radicals. These "$\cdot O_2{}^-$" and "$\cdot$OH" radicals are the key ingredients that must be present for the successful oxidation of NO to the neutral component $NO_3{}^-$. The oxidation of NO is associated with the difference between how much more negative the CB band potential is (than the $O_2/\cdot O_2{}^-$ potential of 0.33 eV) and how considerably positive the VB band potential is (than the $OH^-/\cdot$OH potential of 1.99 eV). The reactions correlate to the generation of radicals, and the following is a plausible route for NO oxidation [6,7,33]:

$$Coated\ Photocatalyst\ (\mathrm{ZT}-01) + h\vartheta \rightarrow \frac{phtogenerated\ e^-}{h^+} pairs \quad (2)$$

$$Reduction\ of\ adsorbed\ O_2 = e^- + O_2 \rightarrow \cdot O_2^- \quad (3)$$

$$Oxidation\ of\ adsorbed\ H_2O = h^+ + OH^- \rightarrow \cdot OH \quad (4)$$

$$\cdot O_2^- + NO \rightarrow NO_3^- \quad (5)$$

$$\cdot OH + NO \rightarrow NO_2 \quad (6)$$

$$\cdot OH + NO_2 \rightarrow NO_3^- \quad (7)$$

4. Conclusions

In this work, the evaluation approach used in the laboratory using specimens was improved in order to provide an assessment strategy that can validate the actual performance of photocatalyst applications in the field. Furthermore, an assessment method was developed to investigate the issue of variances in photocatalyst activity based on sample preparation conditions and on-site photocatalyst application conditions. As the evaluated methods in this study, the standard gas measurement method and the dual reactor measurement method were devised and introduced. By conducting the on-site evaluation, the evaluation method's effectiveness and advantages and disadvantages were reviewed. It was confirmed that the standard gas measurement method could evaluate the photocatalyst applied to the actual outdoor site. It is possible to assess the activation level using sunlight irradiated onto the surface to which the photocatalyst is applied. In addition, it was confirmed that even if the same photocatalyst product was used, there was a difference in photocatalytic activity depending on the applied site characteristics, substrate location, and sunlight irradiation intensity of the site. It was confirmed that the photoactivity of the photocatalyst used outdoors could be evaluated by the standard gas measurement method, and the performance of the photocatalyst installed on different substrates and sites could be compared. However, although the concentration of the incoming NO gas is the same, it is reckoned that an additional experiment under the condition that the light source is kept the same is necessary for the performance comparison of the field where the photocatalyst is applied due to the change in the states of sunlight.

The dual reactor measurement method was confirmed to verify the effect of the ambient condition on the photocatalyst of the site under the same sunlight irradiated condition. It is believed that monitoring can be performed using this method. In addition, when evaluating the activity of a photocatalyst under actual air quality and sunlight irradiation conditions, it is deemed that it can be used as primary data to analyze the photocatalyst field application. However, even if the effect of the applied photocatalyst is excellent and the surrounding air quality is good, the amount of decomposition by the photocatalyst can be measured to be substantially low. The standard gas measurement method and the dual reactor measurement method presented in this study are considered valuable for confirming the effect of the photocatalyst applied to the field and verifying the effect of improving air quality when the photocatalyst is used. However, it can be seen that the presented methods each have their own strengths and weaknesses, and some aspects need to be supplemented. Future work could evaluate whether the weather resistance of the photocatalyst application surface can be assessed through periodic measurement and try to determine the correlation with the existing evaluation method, which is used as a specimen in the laboratory. It is expected that by inferring field applicability via this test method and assessing photocatalyst activity applied to the field, it will be feasible to eliminate trial and error and improve the efficacy of photocatalyst application.

Author Contributions: Conceptualization, H.-J.P. and J.-H.K.; methodology, H.-J.P.; formal analysis, H.-J.P. and S.M.H.; investigation, H.-J.P.; resources, K.C. and J.-H.K.; data curation, H.-J.P. and S.M.H.; writing—original draft preparation, H.-J.P. and S.M.H.; writing—review and editing, K.C., H.-K.S. and J.-H.K.; supervision, H.-K.S. and J.-H.K.; project administration, J.-H.K.; funding acquisition, K.C., H.-K.S. and J.-H.K. All authors have read and agreed to the published version of the manuscript.

Funding: This research was supported by a grant (18SCIP-B145909-01) from Smart Civil Infrastructure Research Program funded by Ministry of Land, Infrastructure, and Transport of the Korean government.

Data Availability Statement: The data used to support the study are included in the article.

Conflicts of Interest: The authors declare no conflict of interest.

References

1. South Korea/Textbar Environmental Performance Index. Available online: https://epi.yale.edu/epi-results/2022/country/kor (accessed on 21 April 2022).
2. Yang, K.-H.; Mun, J.-H. Air Pollutants Removal Rates of Permeable Blocks Embedded with Zeolites. *J. Korea Concr. Inst.* **2022**, *34*, 3–11. [CrossRef]
3. Tobaldi, D.M.; Dvoranova, D.; Lajaunie, L.; Rozman, N.; Figueiredo, B.; Seabra, M.P.; Skapin, A.S.; Calvino, J.J.; Brezova, V.; Labrincha, J.A. Graphene-TiO_2 hybrids for photocatalytic aided removal of VOCs and nitrogen oxides from outdoor environment. *Chem. Eng. J.* **2021**, *405*, 126651. [CrossRef] [PubMed]
4. Tsang, C.H.A.; Li, K.; Zeng, Y.; Zhao, W.; Zhang, T.; Zhan, Y.; Xie, R.; Leung, D.Y.C.; Huang, H. Titanium oxide based photocatalytic materials development and their role of in the air pollutants degradation: Overview and forecast. *Environ. Int.* **2019**, *125*, 200–228. [CrossRef] [PubMed]
5. Hossain, S.M.; Tijing, L.; Suzuki, N.; Fujishima, A.; Kim, J.-H.; Shon, H.K. Visible light activation of photocatalysts formed from the heterojunction of sludge-generated TiO_2 and g-CN towards NO removal. *J. Hazard. Mater.* **2022**, *422*, 126919. [CrossRef]
6. Hossain, S.M.; Park, H.; Kang, H.J.; Mun, J.S.; Tijing, L.; Rhee, I.; Kim, J.H.; Jun, Y.S.; Shon, H.K. Synthesis and NO_x removal performance of anatase S-TiO_2/g-CN heterojunction formed from dye wastewater sludge. *Chemosphere* **2021**, *275*, 130020. [CrossRef]
7. Hossain, S.M.; Park, H.; Kang, H.J.; Mun, J.S.; Tijing, L.; Rhee, I.; Kim, J.H.; Jun, Y.S.; Shon, H.K. Facile synthesis and characterization of anatase TiO_2/g-CN composites for enhanced photoactivity under UV-visible spectrum. *Chemosphere* **2021**, *262*, 128004. [CrossRef]
8. Hossain, S.M.; Park, H.; Kang, H.-J.; Mun, J.S.; Tijing, L.; Rhee, I.; Kim, J.-H.; Jun, Y.-S.; Shon, H.K. Modified Hydrothermal Route for Synthesis of Photoactive Anatase TiO_2/g-CN Nanotubes from Sludge Generated TiO_2. *Catalysts* **2020**, *10*, 1350. [CrossRef]
9. Cros, C.J.; Terpeluk, A.L.; Crain, N.E.; Juenger, M.C.; Corsi, R.L. Influence of environmental factors on removal of oxides of nitrogen by a photocatalytic coating. *J. Air Waste Manag. Assoc.* **2015**, *65*, 937–947. [CrossRef]
10. Kim, M.; Kim, H.; Park, J. Empirical NO_x Removal Analysis of Photocatalytic Construction Materials at Real-Scale. *Materials* **2021**, *14*, 5717. [CrossRef] [PubMed]
11. Kim, J.-H.; Hossain, S.M.; Kang, H.-J.; Park, H.; Tijing, L.; Park, G.W.; Suzuki, N.; Fujishima, A.; Jun, Y.-S.; Shon, H.K.; et al. Hydrophilic/Hydrophobic Silane Grafting on TiO2 Nanoparticles: Photocatalytic Paint for Atmospheric Cleaning. *Catalysts* **2021**, *11*, 193. [CrossRef]
12. Khan, T.; Bari, G.; Kang, H.-J.; Lee, T.-G.; Park, J.-W.; Hwang, H.; Hossain, S.; Mun, J.; Suzuki, N.; Fujishima, A.; et al. Synthesis of N-Doped TiO_2 for Efficient Photocatalytic Degradation of Atmospheric NO_x. *Catalysts* **2021**, *11*, 109. [CrossRef]
13. Yang, L.; Hakki, A.; Zheng, L.; Jones, M.R.; Wang, F.; Macphee, D.E. Photocatalytic concrete for NO_x abatement: Supported TiO_2 efficiencies and impacts. *Cem. Concr. Res.* **2019**, *116*, 57–64. [CrossRef]
14. Song, W.; Zeng, Y.; Wang, Y.; Zhang, S.; Zhong, Q.; Wang, T.; Wang, X. Photo-induced strong active component-support interaction enhancing NO_x removal performance of CeO_2/TiO_2. *Appl. Surf. Sci.* **2019**, *476*, 834–839. [CrossRef]
15. Schwartz-Narbonne, H.; Jones, S.H.; Donaldson, D.J. Indoor Lighting Releases Gas Phase Nitrogen Oxides from Indoor Painted Surfaces. *Environ. Sci. Technol. Lett.* **2019**, *6*, 92–97. [CrossRef]
16. Martinez-Oviedo, A.; Ray, S.K.; Nguyen, H.P.; Lee, S.W. Efficient photo-oxidation of NO_x by Sn doped blue TiO_2 nanoparticles. *J. Photochem. Photobiol. A Chem.* **2019**, *370*, 18–25. [CrossRef]
17. Ketzel, M.; Frohn, L.M.; Christensen, J.H.; Brandt, J.; Massling, A.; Andersen, C.; Im, U.; Jensen, S.S.; Khan, J.; Nielsen, O.-K.; et al. Modelling ultrafine particle number concentrations at address resolution in Denmark from 1979 to 2018–Part 2: Local and street scale modelling and evaluation. *Atmos. Environ.* **2021**, *264*, 118633. [CrossRef]
18. Hingorani, R.; Jimenez-Relinque, E.; Grande, M.; Castillo, A.; Nevshupa, R.; Castellote, M. From analysis to decision: Revision of a multifactorial model for the in situ assessment of NO_x abatement effectiveness of photocatalytic pavements. *Chem. Eng. J.* **2020**, *402*, 126250. [CrossRef]
19. Gopalan, A.-I.; Lee, J.-C.; Saianand, G.; Lee, K.-P.; Sonar, P.; Dharmarajan, R.; Hou, Y.-l.; Ann, K.-Y.; Kannan, V.; Kim, W.-J. Recent Progress in the Abatement of Hazardous Pollutants Using Photocatalytic TiO_2-Based Building Materials. *Nanomaterials* **2020**, *10*, 1854. [CrossRef]
20. Jimenez-Relinque, E.; Hingorani, R.; Rubiano, F.; Grande, M.; Castillo, A.; Castellote, M. In situ evaluation of the NO_x removal efficiency of photocatalytic pavements: Statistical analysis of the relevance of exposure time and environmental variables. *Environ. Sci. Pollut. Res.* **2019**, *26*, 36088–36095. [CrossRef]
21. Cassar, L. Photocatalysis of Cementitious Materials: Clean Buildings and Clean Air. *MRS Bulletin* **2004**, *29*, 328–331. [CrossRef]
22. Boonen, E.; Beeldens, A. Photocatalytic roads: From lab tests to real scale applications. *Eur. Transport. Res. Rev.* **2013**, *5*, 79–89. [CrossRef]
23. Folli, A.; Strøm, M.; Madsen, T.P.; Henriksen, T.; Lang, J.; Emenius, J.; Klevebrant, T.; Nilsson, Å. Field study of air purifying paving elements containing TiO_2. *Atmos. Environ.* **2015**, *107*, 44–51. [CrossRef]
24. Ballari, M.M.; Hunger, M.; Hüsken, G.; Brouwers, H.J.H. NO_x photocatalytic degradation employing concrete pavement containing titanium dioxide. *Appl. Catal. B: Environ.* **2010**, *95*, 245–254. [CrossRef]

25. Gallus, M.; Akylas, V.; Barmpas, F.; Beeldens, A.; Boonen, E.; Boréave, A.; Cazaunau, M.; Chen, H.; Daële, V.; Doussin, J.F.; et al. Photocatalytic de-pollution in the Leopold II tunnel in Brussels: NO_x abatement results. *Build. Environ.* **2015**, *84*, 125–133. [CrossRef]
26. Guerrini, G.L. Photocatalytic performances in a city tunnel in Rome: NO_x monitoring results. *Constr. Build. Mater.* **2012**, *27*, 165–175. [CrossRef]
27. Maggos, T.; Plassais, A.; Bartzis, J.G.; Vasilakos, C.; Moussiopoulos, N.; Bonafous, L. Photocatalytic degradation of NO_x in a pilot street canyon configuration using TiO_2-mortar panels. *Environ. Monit Assess.* **2008**, *136*, 35–44. [CrossRef]
28. Yu, Q.L.; Hendrix, Y.; Lorencik, S.; Brouwers, H.J.H. Field study of NO_x degradation by a mineral-based air purifying paint. *Build. Environ.* **2018**, *142*, 70–82. [CrossRef]
29. de Melo, J.V.S.; Trichês, G.; Gleize, P.J.P.; Villena, J. Development and evaluation of the efficiency of photocatalytic pavement blocks in the laboratory and after one year in the field. *Constr. Build. Mater.* **2012**, *37*, 310–319. [CrossRef]
30. Ballari, M.M.; Brouwers, H.J.H. Full scale demonstration of air-purifying pavement. *J. Hazard. Mater.* **2013**, *254–255*, 406–414. [CrossRef]
31. Cordero, J.M.; Hingorani, R.; Jimenez-Relinque, E.; Grande, M.; Borge, R.; Narros, A.; Castellote, M. NO_x removal efficiency of urban photocatalytic pavements at pilot scale. *Sci. Total Environ.* **2020**, *719*, 137459. [CrossRef]
32. *ISO. 22197-1*; Fine Ceramics (Advanced Ceramics, Advanced Technical Ceramics)—Test Method for Air-Purification Performance of Semiconducting Photocatalytic Materials—Part 1: Removal of Nitric Oxide. ISO: Geneva, Switzerland, 2016.
33. Hossain, S.M.; Park, H.; Kang, H.-J.; Kim, J.B.; Tijing, L.; Rhee, I.; Jun, Y.-S.; Shon, H.K.; Kim, J.-H. Preparation and Characterization of Photoactive Anatase TiO_2 from Algae Bloomed Surface Water. *Catalysts* **2020**, *10*, 452. [CrossRef]